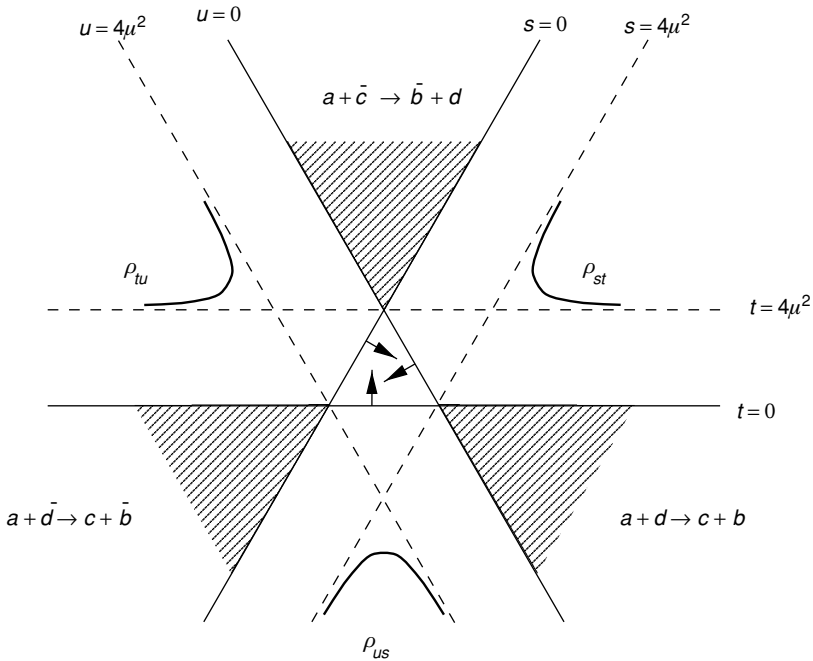# 5
Strong interactions at high energies

5.1 The rôle of cross-channels

In this lecture we return to the study of the four-point amplitude $A(s,t)$. As we already know, it describes three different crossing reactions in the corresponding channels on the Mandelstam plane $s = (p_a + p_b)^2$, $t = (p_a - p_c)^2$, $u = (p_a - p_d)^2$:

In Lecture 3 we examined analytic properties of the amplitude at small energies when, in fact, a small number of partial waves contributed. We discussed that the behaviour of $A(s,t)$ was governed by singularities of these partial waves. We have shown that unitarity led to the appearance of poles on unphysical sheets of the scattering amplitude – resonances – as well as to threshold branch cuts related to these poles. We have also discussed the physical origin of these singularities. Moreover, that was all we could possibly say about the strong interaction since perturbation theory is not applicable in principle (in terms of hadrons, $g^2/4\pi \sim 14$) and the Lagrangian is not known. Even if we knew the underlying Lagrangian, that would not have helped us in calculating amplitudes we were interested in.*

The method we have employed in Lecture 3 fails when we increase the interaction energy because the unitarity condition becomes prohibitively complicated due to the opening of new multi-particle production channels. In spite of this, at *very high* energies s, when the number of inelastic channels becomes large, an interesting new simplification arises in certain regions on the Mandelstam plane.

Take finite $|t|$ and large $s \gg m^2$ and consider *near-to-forward* two-particle scattering at small angles $\Theta_s \sim \sqrt{-t/s} \ll 1$. For $|t| \sim m^2$ it is the nearest singularities in the *t-channel* that will determine the behaviour of the amplitude, while *u*-channel singularities are irrelevant as they lie far away: $|u| \simeq s \gg m^2$. Analogously, we can expect a similar for *near-to-backward* scattering: $|u| \sim m^2$ fixed, $s \to \infty$, in which case a finite number of the nearest *u-channel* singularities will be relevant.

It is clear that the idea of extracting the asymptotic behaviour by means of the *analytic continuation* in the scattering angle variable (either t or u) is bound to be successful. At very large s when the number of the opened inelastic channels is immense, adding one or two would by no means affect the elastic amplitude. Therefore it seems natural to expect that in the $s \to \infty$ limit the t- (or u-) channel unitarity conditions will play a major rôle. This, together with the s-channel unitarity, will allow us to draw a possible picture of strong interactions at high energies.

The key instrument in the realization of this programme will be the *analytic continuation* of the t-channel unitarity condition valid at finite positive $t \sim m^2$ to unphysical scattering angles $\cos\Theta_t \sim s/t \to \infty$ which region is relatively close to that of the physical s-channel scattering, namely, $-t \sim m^2$.

Recall that it is the information coming from *cross-channels* that makes a major difference between the relativistic theory and the usual

---

* Now that we know the Lagrangian – that of QCD – this does not help us much in calculating hadron interaction amplitudes either. (ed.)

non-relativistic quantum mechanics. Still, to better understand the physical peculiarities of strong interactions it is often advisable to turn to non-relativistic theory. Therefore, prior to addressing the specific consequences of the relativistic nature of the theory we shall start our discourse by looking, at a qualitative level, at the main characteristics of an interaction using familiar quantum-mechanical notions. Namely, we will look at the possible behaviour of the interaction *strength* and the interaction *radius* in the asymptotic high-energy regime.

5.2 Qualitative picture of elastic scattering

Consider a four-point amplitude at $s \to \infty$. For the sake of simplicity we will restrict ourselves to the elastic scattering of spinless particles with equal masses μ. From general considerations it is clear that the scattering is concentrated mainly at small angles, in the near-to-forward direction.

At high energy many inelastic channels contribute to the unitarity condition,

$$\mathrm{Im}_s\, A(s,t) \equiv A_1(s,t) = \frac{1}{2} \sum_n \quad \raisebox{1ex}{$A(s+i\varepsilon) \qquad A(s-i\varepsilon)$} \tag{5.1}$$
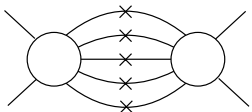
so that at $t = 0$ $(p_1 = p_1',\ p_2 = p_2')$ the imaginary part of the forward amplitude is given by a sum of a large number of positive contributions. According to the optical theorem,

$$\mathrm{Im}\, A(s,0) \simeq s\sigma_{\mathrm{tot}}, \qquad s \gg \mu^2. \tag{5.2}$$

Therefore, if σ_{tot} is constant (or changing slowly) at high energies, which is what experiment tells us, then the forward amplitude increases like s. Let us see what such a behaviour corresponds to in the language of partial waves:

$$\mathrm{Im}\, A(s,t) = \sum_{\ell=0}^{\infty} (2\ell + 1)\, \mathrm{Im}\, f_\ell(s) P_\ell(z), \tag{5.3a}$$

$$z \equiv \cos\Theta_s = 1 + \frac{2\,t}{s - 4\mu^2}. \tag{5.3b}$$

At $t = 0$ we have $P_\ell(1) = 1$. Since from the unitarity condition (3.7) it follows that

$$0 \leq \mathrm{Im}\, f_\ell(s) \leq 16\pi, \tag{5.4}$$

see (3.9), each term in (5.3a) is positive and bounded from above. This means that the growth of the amplitude $A(s, 0) \propto s$ that we are looking for may come only from the increase of the number of terms $\ell_0(s)$ that contribute significantly to the series, $\ell < \ell_0(s)$.

From quantum mechanics we know that high-energy scattering off a finite-range potential with radius ρ_0 is of quasi-classical nature. Therefore we can introduce an impact parameter ρ by identifying

$$\ell = k_c\rho, \tag{5.5}$$

with k_c the cms momentum (3.8),

$$k_c = \frac{\sqrt{s - 4\mu^2}}{2} \simeq \frac{1}{2}\sqrt{s}.$$

Now, to define an interaction radius we equate

$$\ell_0(s) = k_c\rho_0. \tag{5.6a}$$

Since our interaction is *strong* it is natural to expect the partial waves with $\ell < \ell_0$ (that is $\rho < \rho_0$) to be *saturated*,

$$\operatorname{Im} f_\ell(s) = \mathcal{O}(1) \quad \text{for } \ell < \ell_0, \tag{5.6b}$$

and to be negligibly small for $\ell > \ell_0$ when, in the classical language, the projectile misses the target, $\rho > \rho_0$. Now we estimate the size of the imaginary part of the forward elastic amplitude by simply truncating the sum at $\ell \sim \ell_0 \gg 1$:

$$\operatorname{Im} A(s, 0) \sim \ell_0^2 \sim s \cdot \rho_0^2. \tag{5.7}$$

Invoking (5.2) gives then a natural formula for the cross section,

$$\sigma_{\text{tot}} \sim \rho_0^2. \tag{5.8}$$

In the first lecture we discussed the strong interaction characterized by a finite radius which is determined by hadron masses. In a relativistic theory (in marked contrast with non-relativistic quantum mechanics) the 'potential' depends in general on particle velocities. Therefore the interaction radius *may* vary with energy,

$$\rho_0 = \rho_0(s). \tag{5.9}$$

Strictly speaking, the notion of the interaction potential is inapplicable in relativistic theory. Therefore (5.6) in fact serves as a *definition* of the interaction radius through the number of saturated partial waves.

5.2.1 Forward scattering

In the case of $\Theta_s \neq 0$ $(t < 0)$ terms on the r.h.s. of (5.1) enter with different phases and the resulting amplitude decreases fast with $|t|$ increasing: the elastic cross section has a sharp peak in the forward direction.

How could we estimate the range of angles the scattering amplitude is concentrated in? Since essential partial waves have $\ell \sim \ell_0 \gg 1$, characteristic scattering angles can be estimated as

$$\Theta < \Theta_0 \ \sim \ \frac{1}{\ell_0} \ \sim \ \frac{1}{k_c \rho_0} \ll 1. \tag{5.10}$$

The cms momentum transfer at high energies is

$$|\mathbf{q}| = \left| \mathbf{p}_1' - \mathbf{p}_1 \right| \ \sim \ k_c \Theta_0 \sim \ \frac{1}{\rho_0}. \tag{5.11}$$

This means that in terms of Mandelstam variables the amplitude is concentrated in the region of finite momentum transfers, $|t| \ \sim \ 1/\rho_0^2$.

5.2.2 Backward peak

The qualitative expectation is that the scattering at *finite* angles is suppressed in the $s \to \infty$ limit holds provided the factor $\mathrm{Im}\, f_\ell$ in the expansion (5.3a) is a smooth function of ℓ. That was the case in non-relativistic quantum mechanics (where ℓ enters analytically the centrifugal term of the Hamiltonian). In the relativistic theory, on the contrary, $\mathrm{Im}\, f_\ell$ *oscillates* with ℓ and this leads to a new, interesting phenomenon – the appearance of the second narrow peak in the *backward* direction ($\pi - \Theta \ll 1$).

To single out this oscillating behaviour of $\mathrm{Im}\, f_\ell$ we need to employ analytic properties of $A(s,t)$. To this end it is convenient to express the partial wave $f_\ell(s)$ defined by (3.10) in terms of the function

$$Q_\ell(z) \ \equiv \ \frac{1}{2} \int_{-1}^{1} \frac{dz'\, P_\ell(z')}{z - z'}, \tag{5.12}$$

representing the second solution of the Legendre equation, regular at infinity:

$$Q_\ell(z) \ \overset{|z| \to \infty}{\sim} \ z^{-\ell-1}.$$

From (5.12) it immediately follows that $Q_\ell(z)$ has a logarithmic branch cut between -1 to $+1$. Discontinuity over the cut returns the P_ℓ function:

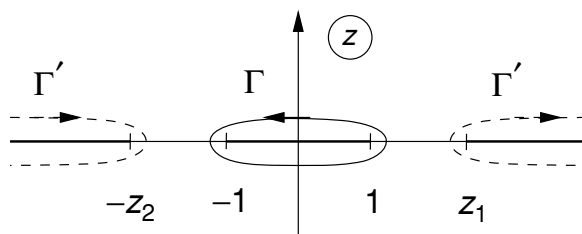$$Q_\ell(z + \imath\epsilon) - Q_\ell(z - \imath\epsilon) = -i\pi P_\ell(z), \quad -1 < z < 1. \tag{5.13}$$

Fig. 5.1 Change of the integration contour $\Gamma \to \Gamma'$ in the representation (5.14) for the partial-wave amplitude.

Using this fact we can replace integration over real z by a contour integral

$$\int_{-1}^{1} dz\, P_\ell(z) \cdots = \frac{1}{\pi i} \int_\Gamma dz\, Q_\ell(z) \cdots ,$$

where Γ runs clock-wise embracing the interval $[-1, 1]$ as displayed in Fig. 5.1. This allows us to represent the partial-wave amplitude as

$$f_\ell(s) = \int_{-1}^{1} dz\, P_\ell(z) A(s, z) = \frac{1}{2\pi i} \int_\Gamma dz\, Q_\ell(z) A(s, z). \qquad (5.14)$$

We took the liberty of replacing the second argument of the amplitude t by the cosine of the scattering angle (5.3b); the two variables, when s is kept fixed, are simply proportional. Now we look at the analytic features of the amplitude. As a functions of t it has two unitarity cuts corresponding to the opening of t- and u-channel thresholds, $t \geq t_{\min}$ and $u \geq u_{\min}$, respectively. In the z plane they translate into the cuts

$$z_1 < z < +\infty; \qquad z_1 = 1 + \frac{2 \cdot t_{\min}}{s - 4\mu^2}; \qquad (5.15a)$$

$$-\infty < z < -z_2; \qquad z_2 = 1 + \frac{2 \cdot u_{\min}}{s - 4\mu^2}. \qquad (5.15b)$$

(In our toy model where all particles are identical, $t_{\min} = u_{\min} = (2\mu)^2$.) Since Q_ℓ falls on the large circle, $|z| \to \infty$, we can deform and replace Γ by another contour Γ' which runs around the left and right cuts as shown in Fig. 5.1. This gives us

$$f_\ell(s) = \frac{1}{\pi} \int_{z_1}^{\infty} dz\, Q_\ell(z) A_3(s, z) + \frac{1}{\pi} \int_{-z_2}^{-\infty} dz\, Q_\ell(z) A_2(s, z), \qquad (5.16)$$

where $A_3 = \mathrm{Im}_t A$ and $A_2 = \mathrm{Im}_u A$ denote discontinuities ('imaginary parts') of the amplitude $A(s, t)$ in the t and u channels. Using the relation
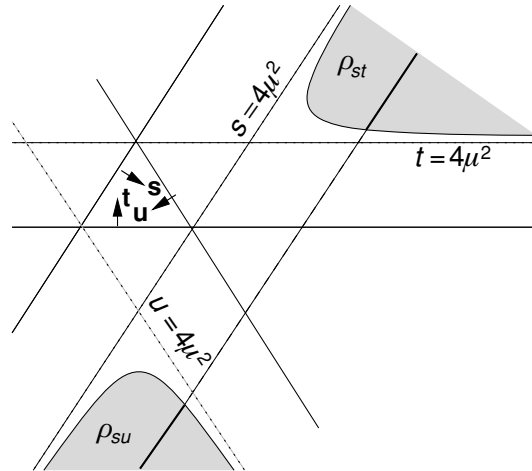
Fig. 5.2   Integration over double spectral functions ρ_{st} and ρ_{su} determining the imaginary part of the partial wave, $\operatorname{Im} f_\ell(s)$, in (5.20).

(valid for integer ℓ)

$$Q_\ell(-z) = (-1)^{\ell+1} Q_\ell(z), \tag{5.17}$$

we may rewrite (5.16) in the following form ($z_u = -z$):

$$f_\ell(s) = \frac{1}{\pi} \int_{z_1}^{\infty} dz\, Q_\ell(z) A_3(s,z) + \frac{(-1)^\ell}{\pi} \int_{z_2}^{\infty} dz_u\, Q_\ell(z_u) A_2(s,-z_u). \tag{5.18}$$

Evaluating the imaginary part of the partial wave, we obtain

$$\operatorname{Im} f_\ell \;=\; \operatorname{Im} f_\ell^{\mathrm{right}} + (-1)^\ell \operatorname{Im} f_\ell^{\mathrm{left}}, \tag{5.19}$$

where

$$\operatorname{Im} f_\ell^{\mathrm{right}}(s) \;=\; \frac{1}{\pi} \int_{z_1}^{\infty} dz\, Q_\ell(z) \rho_{st}(s,t(z)), \tag{5.20a}$$

$$\operatorname{Im} f_\ell^{\mathrm{left}}(s) \;=\; \frac{1}{\pi} \int_{z_2} dz\, Q_\ell(z) \rho_{su}(s,u(-z)). \tag{5.20b}$$

It is worth noticing that the imaginary part of the partial wave is determined by discontinuities across the Landau singularities – spectral functions ρ_{st} and ρ_{su} as shown in Fig. 5.2. Contributions of the right and left cuts in the t-plane (5.20) are smooth functions of ℓ. The oscillating factor $(-1)^\ell$ is explicitly written in (5.19) so now we are ready to return to the partial-wave expansion (5.3a) and scan through all angles to see what happens to the amplitude.

$\boldsymbol{\theta \simeq 0}$. In the forward direction we have $z \simeq 1$ and $P_\ell(1) = 1$.

$$A_1(s, z=1) = \sum_\ell (2\ell + 1) \operatorname{Im} f_\ell^{\text{right}} + \sum_\ell (-1)^\ell \cdot (2\ell + 1) \operatorname{Im} f_\ell^{\text{left}}.$$

The contribution of the left cut is small (of the order of a single partial wave) and the large contribution $\propto s$ is coming from the right cut.

$\boldsymbol{\theta \simeq \frac{\pi}{2}}$. For large angles $z \simeq 0$ so that $P_{2n+1}(0) \simeq 0$ and, for large n, $P_{2n}(0) \simeq \frac{2(-1)^n}{\sqrt{\pi n}}$. We obtain

$$A_1(s, z=0) \simeq \sum_{\ell=2n} (-1)^n \cdot \frac{2(4n+1)}{\sqrt{\pi n}} \left(\operatorname{Im} f_{2n}^{\text{right}} + \operatorname{Im} f_{2n}^{\text{left}} \right).$$

The series is oscillating, resulting in $A_1 = \mathcal{O}(1) \ll s$.

$\boldsymbol{\theta \simeq \pi}$. For backward scattering, $z \simeq -1$, $P_\ell(-1) = (-1)^\ell$. Here

$$A_1(s, z=-1) = \sum_\ell (-1)^\ell \cdot (2\ell + 1) \operatorname{Im} f_\ell^{\text{right}} + \sum_\ell (2\ell + 1) \operatorname{Im} f_\ell^{\text{left}}$$

and, contrary to NQM, we have again a same-sign series which originates this time from the *left* cut of the relativistic amplitude.

The qualitative behaviour of the amplitude as a function of the scattering angle is shown in Fig. 5.3.

If particles are *identical* then 'forward' and 'backward' directions are indistinguishable so that the scattering amplitude becomes obviously symmetric, $A(\Theta) = A(\pi - \Theta)$, both in relativistic and non-relativistic theories. However, if participating particles are different, then from the point of view of NQM this situation looks totally bizarre.

Why would a 180° scattering – the full reflection of particle momenta – be profitable? In NQM, to encourage backward scattering one would have
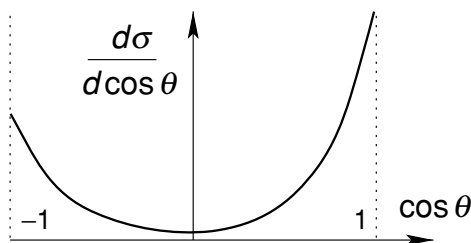

Fig. 5.3   Angular dependence of relativistic two particle scattering.

to organize a head-on collision whose probability is falling with energy as

$$\sigma \propto \lambda^2 \sim 1/s \tag{5.21}$$

(with λ the cms wavelength $\lambda \sim 1/k_c$). The answer lies in the following consideration.

In a relativistic theory the 'potential' may carry quantum numbers. Therefore there is another possibility as an alternative to the large momentum transfer: rather then exchanging *momenta*, colliding particles may swap their *identities* instead. This means that by nature the backward scattering phenomenon is not different from diffractive scattering which is characterized by finite momentum transfer, but accompanied by an exchange of quantum numbers!

Have we ever met such a phenomenon before? In fact we have. Recall the Compton scattering in QED. In the leading order of perturbation theory we had two contributing Feynman diagrams,
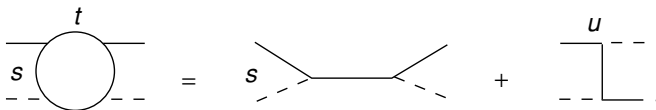
In the $s \to \infty$ limit the first amplitude becomes negligible. It corresponds to interaction in a single partial wave – a head-on collision – so that the qualitative estimate (5.21) applies. At the same time the second amplitude describes a peripheral interaction with finite momentum transfer $|u| \sim m_e^2$ so that high-energy electron–photon scattering occurs mostly backwards ($s \simeq |t| \gg |u|$).

5.3 Analyticity of elastic amplitude and interaction radius

Let us study the ℓ-dependence of partial waves $f_\ell(s)$. We know that in the physical region of the s-channel $A(s, t)$ has no singularities. Therefore the partial-wave expansion series

$$A(s, t) = \sum_{\ell=0}^{\infty} (2\ell + 1) f_\ell(s) P_\ell(z) \tag{5.22}$$

must be absolutely converging, together with all its derivatives. To ensure such a regularity, f_ℓ must decrease fast with ℓ in the $\ell \to \infty$ limit.

5.3.1 f_ℓ at large ℓ

At the first sight a power falloff would seem to be sufficient since at large ℓ

$$P_\ell(z) \simeq J_0(\ell\Theta) \simeq \sqrt{\frac{2}{\pi\ell}}\, \cos\left(\ell\Theta - \frac{\pi}{4}\right); \tag{5.23}$$

$$\ell \gg 1, \quad \Theta \ll 1, \quad \ell\Theta = \mathcal{O}(1)\,.$$

We know, however, that the series must stay convergent in the unphysical region of positive t as well, up to $t = t_0$ where the first t-channel singularity is positioned (for example, $t_0 = 4m_\pi^2$ for $\pi\pi \to \pi\pi$ scattering). According to (5.3b), $t > 0$ corresponds to $z > 1$ where the scattering angle is imaginary,

$$z = \cos\Theta = 1 + \frac{2\,t}{s - 4m_\pi^2} = \cosh\chi, \quad \Theta = i\chi, \tag{5.24}$$

and the Legendre polynomials start to grow exponentially with ℓ:

$$P_\ell(z) \sim \mathrm{e}^{i\ell\Theta} + \mathrm{e}^{-i\ell\Theta} \sim \mathrm{e}^{\ell\chi(t,s)}. \tag{5.25}$$

Up to $t \leq t_0$, this increase has to be damped by the fall-off of partial waves. Consequently,

$$f_\ell(s) \stackrel{\ell \gtrsim 1}{\simeq} C(\ell, s)\, \mathrm{e}^{-\ell\chi_0}, \tag{5.26a}$$

where the factor C is non-exponential in ℓ and

$$\cosh\chi_0 \equiv 1 + \frac{2 \cdot t_0}{s - 4m_\pi^2}. \tag{5.26b}$$

In the $s \to \infty$ limit we have

$$\cosh\chi_0 \simeq 1 + \frac{\chi_0^2}{2} \to 1, \quad \chi_0 \simeq \sqrt{\frac{4t_0}{s}} \simeq \frac{\sqrt{t_0}}{k_c}. \tag{5.27}$$

In terms of the impact parameter (5.5), $\rho = \ell/k_c$, the large-ℓ asymptotic regime (5.26) takes the form

$$f_\ell(s) \implies f(\rho, s) = C(\rho, s)\, \mathrm{e}^{-\rho/r_0}, \quad r_0 \equiv 1/\sqrt{t_0}. \tag{5.28}$$

In particular, for $\pi\pi$ scattering ($t_0 = 4m_\pi^2$) the condition (5.27) gives

$$\chi_0 \simeq \frac{2m_\pi}{k_c} \quad \text{and} \quad r_0 = \frac{1}{2m_\pi}.$$

We conclude that partial waves with large ℓ that correspond to impact parameters ρ exceeding the interaction radius, $\rho \gg \rho_0$, fall exponentially as $\exp(-\rho/r_0)$.

It is important to stress that the nature of the two parameters ρ_0 and r_0 is essentially different: the radius ρ_0 we have introduced in (5.6a) as a
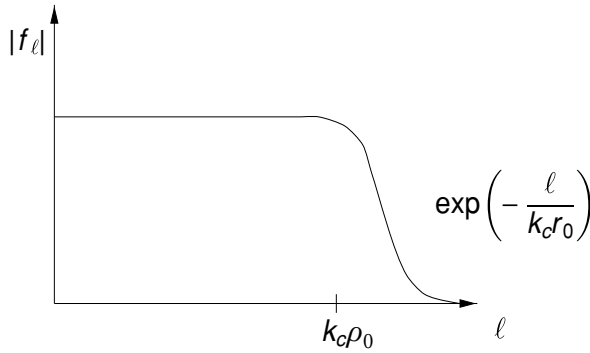
Fig. 5.4 Qualitative picture of the magnitude of partial waves.

measure of the of the *value* of characteristic angular momentum ℓ_0 below which partial waves are saturated, while r_0 determines the rate of the falloff of small partial waves with $\ell \gg \ell_0$, see Fig. 5.4.

5.3.2 Black disc

What can be said about partial-wave amplitudes below ℓ_0? It is impossible to answer this question without knowing the details of strong interaction dynamics. Nevertheless, it is straightforward to give an estimate *from above* for elastic, inelastic and total cross sections at high energies.

In Lecture 3 we discussed elastic unitarity for partial waves. Above the two-particle threshold the elastic unitarity condition (3.7) generalizes as

$$\operatorname{Im} f_\ell = \tau |f_\ell|^2 + \Delta_\ell, \tag{5.29}$$

where $\Delta_\ell \geq 0$ accounts for contribution of inelastic scattering channels: $2 \to 3$, $2 \to 4$, etc. The general solution for partial waves reads

$$f_\ell(s) = \frac{1}{2i\tau(s)} \left[\eta_\ell(s) \, e^{2i\delta_\ell(s)} - 1 \right], \tag{5.30a}$$

where η_ℓ is the so-called elasticity parameter,

$$\eta_\ell^2 = 1 - 4\tau\Delta_\ell, \qquad 0 \leq \eta_\ell \leq 1. \tag{5.30b}$$

Elastic unitarity corresponds to

$$\eta_\ell = 1, \qquad \Delta_\ell \equiv 0. \tag{5.31a}$$

On the contrary, at very high energies when inelastic channels dominate the unitarity condition it is natural to expect

$$\eta_\ell \simeq 0, \qquad \Delta_\ell \simeq \Delta_{\max} \simeq 4\pi. \tag{5.31b}$$

Invoking the optical theorem (5.2) we have

$$\sigma_{\text{tot}} \;=\; \frac{1}{s} \sum_{\ell} (2\ell + 1)\, \text{Im}\, f_\ell \tag{5.32}$$

and, using (5.30a), for the total cross section obtain

$$\sigma_{\text{tot}} \simeq \frac{1}{2\tau s} \sum_{\ell}^{\ell_0} (2\ell + 1)\left[\, 1 - \eta_\ell \cos(2\delta_\ell)\, \right]. \tag{5.33a}$$

Then, integrating over angles the elastic amplitude squared, it is straightforward to derive

$$\sigma_{\text{el}} \simeq \frac{1}{4\tau s} \sum_{\ell}^{\ell_0} (2\ell + 1)\left[\, 1 - 2\eta_\ell \cos(2\delta_\ell) + \eta_\ell^2\, \right]. \tag{5.33b}$$

Finally, from $\sigma_{\text{tot}} = \sigma_{\text{el}} + \sigma_{\text{in}}$ we get the total *inelastic* cross section,

$$\sigma_{\text{in}} \simeq \frac{1}{4\tau s} \sum_{\ell}^{\ell_0} (2\ell + 1)\left[\, 1 - \eta_\ell^2\, \right]. \tag{5.33c}$$

The maximal value of $\text{Im}\, f_\ell$ in (5.32) can be estimated as

$$[\text{Im}\, f_\ell(s)]^{\text{max}} \;=\; \frac{1}{2\tau(s)} \simeq 8\pi\,, \tag{5.34}$$

where we dropped the exponential term in (5.30a): it is unrealistic to expect that all scattering phases with large ℓ are artificially adjusted so that this oscillating contribution will matter. This gives the upper boundary

$$\sigma_{\text{tot}} \;\leq\; [\sigma_{\text{tot}}]^{\text{max}} \simeq \frac{8\pi}{s} \cdot \ell_0^2 \simeq 2\pi\rho_0^2. \tag{5.35}$$

If we accept the natural *maximal inelasticity* hypothesis (5.31b), then the relations (5.33) give

$$\sigma_{\text{el}} = \sigma_{\text{in}} = \tfrac{1}{2}\sigma_{\text{tot}} \;=\; \pi\rho_0^2\,. \tag{5.36}$$

This corresponds to the well-known quantum-mechanical picture of scattering off a black disc of radius ρ_0: half of σ_{tot} is inelastic and corresponds to the geometrical cross section of a fully absorbing disc (impact parameters $\rho \leq \rho_0$) while the other half is due to the elastic diffraction of the plane wave (at $\rho > \rho_0$) off the sharp edge of the disc.

Let us make a few additional remarks.

(1) The exponential falloff of partial waves at $\ell \gg 1$ is related to the absence of *massless particles* in the theory.

(2) The concrete value of r_0 is different for different reactions. For $\pi\pi$ scattering we had $r_0 = 1/2m_\pi$. For nucleon scattering we would have $t_0 = m_\pi^2$ and $r_0 = 1/m_\pi$ instead since there is a pion pole in the amplitude of the t-channel reaction $N\bar{N} \to \pi \to N\bar{N}$.

5.3.3 Behaviour of $\operatorname{Im} f_\ell$ at large ℓ

With the help of (5.26) and the unitarity relation (3.7) we can verify that, as we have seen in Lecture 2, the behaviour of $\operatorname{Im} A(s,t)$ is governed not by physical t-channel poles and/or thresholds but by the *Landau–Mandelstam singularities*.

Indeed, in the finite energy region of $\pi\pi$ scattering $4m_\pi^2 < s < 16m_\pi^2$ where inelastic channels are 'closed' ($\Delta_\ell \equiv 0$, $\eta_\ell \equiv 1$),

$$\operatorname{Im} f_\ell \ = \ \tau|f_\ell|^2 \sim \mathrm{e}^{-2\cdot\ell\chi_0}, \quad \ell \gg 1. \tag{5.37}$$

As a result, the series (5.3) for $\operatorname{Im} A(s,t)$ will stay convergent *above* $t_0 = 4m_\pi^2$. The critical value of t at which $\operatorname{Im} A$ will develop a singularity will be determined not by $\chi(t,s) = \chi_0$ as for the amplitude A itself but by the condition $\chi(t,s) = 2 \cdot \chi_0$:

$$\cosh\chi = 2\cosh^2\chi_0 - 1; \ 1 + \frac{2t}{s - 4m_\pi^2} = 2\left(1 + \frac{2\cdot 4m_\pi^2}{s - 4m_\pi^2}\right)^2 - 1. \tag{5.38}$$

From (5.38) follows the relation

$$(s - 4m_\pi^2)(t - 16m_\pi^2) \ = \ 64m_\pi^2. \tag{5.39}$$

This is nothing but the Landau–Mandelstam equation describing the position of the singularity – one of the Karplus curves shown in Fig. 5.5 that corresponds to the double discontinuity ρ_{st} of the graph (5.40). Let me remind you that the 'box' graph that we studied in Lecture 2 (with two instead of four lines in the intermediate t-channel state) is absent for true pions since a pion cannot transfer into a $\pi\pi$ system due to G-parity conservation. (We

$$\tag{5.40}$$

excluded another graph similar to (5.40) but with two vertical and four horizontal lines by having chosen $s < 16m_\pi^2$.)
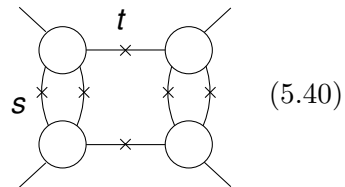
Thus the behaviour of the *imaginary part* of the scattering amplitude, $\operatorname{Im} A$, is determined by the first Landau–Mandelstam singularity $t_i(s)$ given by (5.39) rather than by t_0 as the amplitude A itself. At high energies the difference between $t_i(s)$ and t_0 is, however, washed away. Indeed, already for $s > (4m_\pi)^2$ a two-π state in the t channel becomes allowed and the corresponding Karplus curve on Fig. 5.5 appears. Since *all* Karplus
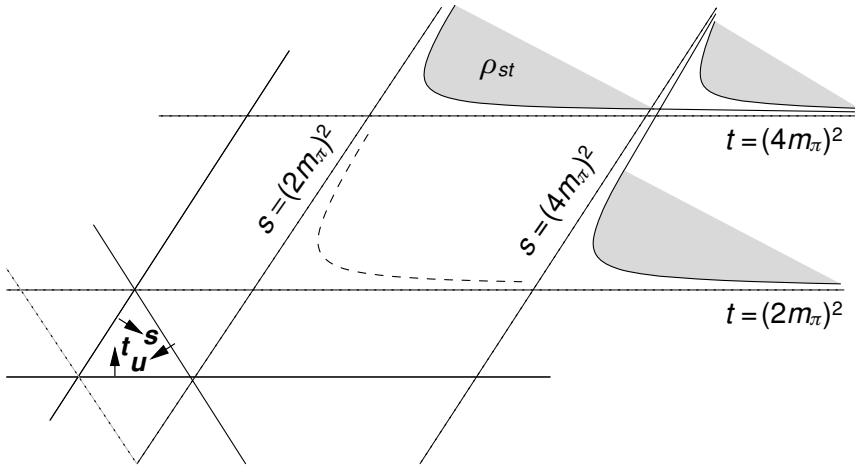
Fig. 5.5   Karplus curves for two- and four-pion states in s- and t-channel. The curve marked ρ_{st} corresponds to (5.39). The Landau–Mandelstam singularity shown by dashed line is absent for $\pi\pi$ scattering.

curves corresponding to two-pion exchange in the t-channel (and any number of particles in the s-channel) tend to the same value $t_i(s) \to (2m_\pi)^2 = t_0$ in the high-energy limit, we get

$$\operatorname{Im} f_\ell \sim f_\ell \sim \mathrm{e}^{-\ell\chi_0} \simeq \mathrm{e}^{-2m_\pi\rho}, \quad s \to \infty.$$

5.4 Impact parameter representation

We will find it convenient to use the impact parameter representation in what follows. So let us look into the physical meaning of partial-wave amplitudes $f_\ell(s) = f(\rho, s)$ in the $\boldsymbol{\rho}$-space.

For fixed $t = -\mathbf{q}^2$ and large s-scattering occurs at small angles $\Theta \simeq \sqrt{-t/s} \ll 1$. The momentum transfer $\mathbf{q}$ is then orthogonal to the cms momentum of incident pions, $\mathbf{q} \perp \mathbf{k}_c$, $q \simeq k_c\Theta$. For small angles the following approximation applies:

$$P_\ell(\cos\Theta) \simeq J_0(\ell\Theta).$$

Since in the partial-wave expansion large ℓ are essential, we can replace the sum in (5.22) by the integral,

$$A(s, q^2) \simeq \int 2\ell d\ell f_\ell(s) P_\ell(\cos\Theta) \simeq k_c^2 \int 2\rho d\rho f(\rho, s) J_0(q\rho), \qquad (5.41)$$

and make use of the integral representation

$$J_0(q\rho) = \int \frac{d\phi}{2\pi} \, \mathrm{e}^{i(\mathbf{q}\cdot\boldsymbol{\rho})}, \qquad (\mathbf{q}\cdot\boldsymbol{\rho}) \equiv q\rho \cdot \cos\phi \qquad (5.42)$$

to arrive at a well-known quantum-mechanical formula

$$A(s, q^2) = \frac{k_c^2}{\pi} \int d^2\boldsymbol{\rho} \, \mathrm{e}^{i(\mathbf{q}\cdot\boldsymbol{\rho})} f(\boldsymbol{\rho}, s). \qquad (5.43)$$

The amplitude (5.43) in NQM describes the following scattering process. Consider a plane wave propagating along the z-axis and hitting the target at $z = 0$. Right behind the target the wave function will be modified by the factor $\lambda(\rho)$ describing the absorption of the incident wave at a given impact parameter,

$$\psi_{\mathrm{out}}(z, \boldsymbol{\rho})|_{z=+0} = \psi_{\mathrm{in}}(z, \boldsymbol{\rho}) \cdot \lambda(\rho), \quad \psi_{\mathrm{in}}(z, \boldsymbol{\rho}) = \mathrm{e}^{ikz}. \qquad (5.44)$$

For example, for a totally absorbing sharp-edge target (a 'black disc' of radius R_0)

$$\lambda(\rho) = \vartheta(\rho - R_0).$$

On the other hand, the plane wave expansion of the final field that we observe at large distance from the target is given by

$$\psi_{\mathrm{out}} = \psi_{\mathrm{in}} \cdot \int d^2\mathbf{q} \, \mathrm{e}^{i(\mathbf{q}\cdot\boldsymbol{\rho})} a(q), \qquad (5.45)$$

where $a(q)$ is the scattering amplitude. Comparing (5.45) at $z = +0$ with (5.44) and inverting the Fourier representation (5.43) we conclude that $f(\boldsymbol{\rho}, s)$ has the meaning of the impact parameter distribution of the field right behind the target.

5.5 Constant interaction radius hypothesis

We found above that the partial-wave amplitude at large ρ has a structure

$$f(\rho, s) = C(\rho, s) \, \mathrm{e}^{-2m_\pi \rho} \qquad (5.46)$$

with C a non-exponential function of ρ. This factor may depend on its two variables in a rather complicated way so that the interaction radius may turn out to be energy-dependent, $\rho_0 = \rho_0(s)$. This is what happens in reality. However, before discussing seriously this phenomenon, it is natural to look at the consequences of the hypothesis of a constant radius:

$$\rho_0(s) = \mathrm{const}.$$

5.5.1 Consequences of the hypothesis $\rho_0(s) = const$

It is easy to convince oneself that this hypothesis actually means that the C-factor in (5.46) *factorizes*:

$$C(\rho, s) = c(\rho\mu) \cdot h(s/\mu^2). \tag{5.47}$$

Indeed, if the functional dependence on ρ and s *did not* separate, the impact parameter distribution of the field would be changing with energy.

What are the main consequences of the hypothesis (5.47)? They are

$$A_{\text{el}}(s,t) = ish(s) \cdot F(t), \tag{5.48a}$$

$$\sigma_{\text{tot}} = \frac{\text{Im}\, A(s,0)}{s} = h(s)F(0), \tag{5.48b}$$

$$\frac{d\sigma_{\text{el}}}{dt} = \frac{1}{16\pi}\left|\frac{A_{\text{el}}(s,t)}{s}\right|^2 = \frac{\sigma_{\text{tot}}^2}{16\pi}\cdot\left|\frac{F(t)}{F(0)}\right|^2. \tag{5.48c}$$

From (5.48c) we conclude that the constant radius implies an energy-independent *shape* of the differential elastic scattering cross section:

$$\frac{1}{\sigma_{\text{tot}}^2(s)}\frac{d\sigma_{\text{el}}(s,t)}{dt} = \text{const}(s).$$

A constant radius is also consistent with the *Pomeranchuk theorem* (Pomeranchuk, 1958).

5.5.2 Pomeranchuk theorem

Consider the scattering of a particle a and its antiparticle $\bar{a}$ on the same target b. If the total cross sections are asympotically constant,

$$\lim_{s\to\infty}\sigma_{\text{tot}}^{ab}(s) = \sigma_a \quad \text{and} \quad \lim_{s\to\infty}\sigma_{\text{tot}}^{\bar{a}b}(s) = \sigma_{\bar{a}},$$

then

$$\sigma_a = \sigma_{\bar{a}}.$$

This is a non-trivial statement as it has nothing to do with charge conjugation invariance: $\sigma_{\text{tot}}^{ab} = \sigma_{\text{tot}}^{\bar{a}\bar{b}}$. The isotopic structure of ab- and $\bar{a}b$-scattering amplitudes may be absolutely different as, for example, is the case of pp and $p\bar{p}$ interactions. Experimentally, cross sections of particle and antiparticle interactions with a given target hadron differ remarkably at moderate energies but become practically equal already at energies s above few hundred GeV^2 (see below, Fig. 14.3 on page 378).

Let us sketch the idea of the proof. Discontinuities of the amplitude on the left and right cuts cannot be different if we want $A(s,t)$ to be

"regular" at infinity. Indeed, let

$$\operatorname{Im} A_{ab}(s,0) \overset{s\to\infty}{=} \sigma_a s,$$
$$\operatorname{Im} A_{\bar{a}b}(u,0) \overset{u\to\infty}{=} \sigma_{\bar{a}} u. \tag{5.49}$$

If the cross sections are different, $\sigma_a \neq \sigma_{\bar{a}}$, then the *real parts* $\operatorname{Re} A$ corresponding to discontinuities (5.49),

$$A_{\text{right}}(s) \simeq \frac{\sigma_a s}{\pi} \ln(-s), \qquad A_{\text{left}}(s) \simeq \frac{\sigma_{\bar{a}} u}{\pi} \ln(-u), \tag{5.50}$$

will not compensate one another:

$$A_{ab}(s) \overset{s\to\infty}{=} A_{\text{right}}(s) + A_{\text{left}}(-s) = i\sigma_a s + \frac{\sigma_a - \sigma_{\bar{a}}}{\pi} \cdot s \ln s,$$
$$A_{\bar{a}b}(u) \overset{u\to\infty}{=} A_{\text{right}}(-u) + A_{\text{left}}(u) = i\sigma_{\bar{a}} u + \frac{\sigma_a - \sigma_{\bar{a}}}{\pi} \cdot u \ln u. \tag{5.51}$$

The amplitudes (5.51) contradict the initial assumption of the theorem (namely, $\sigma_{\text{tot}} = \text{const.}$) as they produce

$$\sigma_{\text{el}}(s) \propto (\sigma_a - \sigma_{\bar{a}})^2 \ln^2 |s| \overset{|s|\to\infty}{\gg} \sigma_{\text{tot}} = \text{const.}$$

Does the Pomeranchuk theorem teach us anything about $f(\rho, s)$ and, specifically, about the interaction radius? In other words, to what extent does the asymptotic equality $\sigma_a = \sigma_{\bar{a}}$ depend on the hypothesis of the constant radius ρ_0?

Let us see how the logarithmic growth of $\operatorname{Re} A$, which is necessary for the theorem to be broken, could appear in principle:

$$\operatorname{Re} A(s,0) = \frac{s}{4\pi} \int d^2\boldsymbol{\rho} \, \operatorname{Re} f(\rho, s). \tag{5.52}$$

From the unitarity condition (5.29) ($\tau \simeq 1/16\pi$ for $s \gg \mu^2$) we have

$$\operatorname{Im} f = \frac{1}{16\pi} |f|^2 + \Delta > \frac{1}{16\pi} |\operatorname{Re} f|^2,$$

which gives

$$\operatorname{Re} f(\rho, s) < \sqrt{16\pi \operatorname{Im} f(\rho, s)}. \tag{5.53}$$

On the other hand, to violate the Pomeranchuk theorem we have to have

$$\operatorname{Re} f(\rho, s) \sim \operatorname{Im} f(\rho, s) \cdot \ln s \tag{5.54}$$

in the essential integration region $\rho \lesssim \rho_0(s)$. Combining (5.53) and (5.54) produces

$$\operatorname{Im} f < \frac{\text{const}}{\ln^2 s}. \tag{5.55}$$

Wishing to preserve the constancy of the total cross section,

$$\sigma_{\text{tot}} = \frac{1}{4\pi} \int d^2\boldsymbol{\rho} \, \text{Im} \, f(\rho, s) \; = \; \rho_0^2 \cdot \frac{\langle \text{Im} \, f \rangle}{4}, \tag{5.56}$$

and taking into consideration the inequality (5.55), we arrive at the necessity to abandon the constant radius, $\rho_0(s) \gtrsim c \ln s$. We shall learn soon that the radius *cannot grow faster* than $\ln s$. This means that only in the extreme case of the fastest possible growth of the interaction radius, $\rho_0(s) \propto \ln s$, the Pomeranchuk theorem may fail.

5.6 Possibility of a growing interaction radius

We discussed the case when the interaction radius, and thus the shape of the elastic peak, does not change with energy, the amplitude factorizes and the Pomeranchuk theorem holds. In the next lecture we shall formally demonstrate that the $\rho_0 = $ const regime is actually forbidden as it contradicts t-channel unitarity.

Let us ask ourselves, whether we can force the radius to grow with energy? What sort of physical processes might be responsible for that, at a qualitative level? Strangely enough, such a possibility does exist.
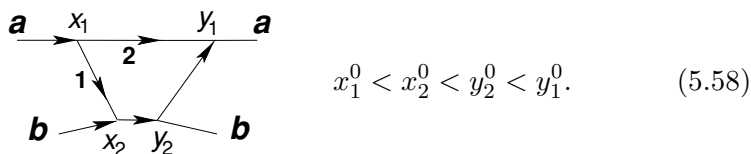
Recall that in perturbative language we have obtained the constant radius $\rho_0 \sim 1/2\mu$ by considering the nearest singularity in t of the amplitude; two-meson t-channel exchange gave us
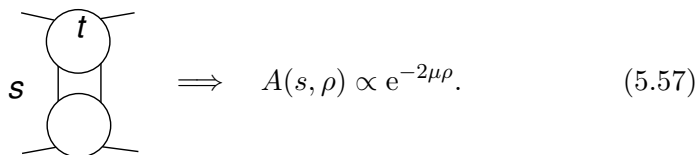
$$\implies \quad A(s, \rho) \propto e^{-2\mu\rho}. \tag{5.57}$$

5.6.1 Long-living fluctuations and the growing radius

Let us study the space–time structure of the simplest perturbative diagram corresponding to the processes (5.57):

$$x_1^0 < x_2^0 < y_2^0 < y_1^0. \tag{5.58}$$

The process (5.58) can be 'spelled out' in time as follows. First, the projectile particle a experienced a virtual decay at the point x_1; one of its offspring at x_2 hit and excited the target b which, in its turn, decayed in

y_2, ... How far can a virtual particle migrate in the transverse plane? From the uncertainty relation, during the lifetime of the fluctuation,

$$\Delta t \sim \Delta E^{-1} \sim \mu^{-1}, \tag{5.59a}$$

a virtual particle k_1 may shift in the transverse plane at a distance

$$|\mathbf{x}_{2\perp} - \mathbf{x}_{1\perp}| \sim \mu^{-1}. \tag{5.59b}$$

Could we allow it to move farther than that so as to make the interaction radius growing? At the first sight this seems to be an easy thing to do: by minimizing the energy uncertainty we may increase the lifetime t in (5.59a) significantly. In the laboratory frame where the particle a is fast and has a very large momentum $p \equiv p_z \simeq s/2\mu \gg \mu$, virtual splitting $a \to 1 + 2$ introduces energy uncertainty

$$
\begin{aligned}
\Delta E &= E_{\text{interm}} - E_{\text{init}} = \sqrt{\mathbf{k}_1^2 + \mu^2} + \sqrt{\mathbf{k}_2^2 + \mu^2} - \sqrt{\mathbf{p}^2 + \mu^2} \\
&\simeq \frac{\mathbf{k}_{1\perp}^2 + \mu^2}{2k_{1z}} + \frac{\mathbf{k}_{2\perp}^2 + \mu^2}{2k_{2z}} - \frac{\mu^2}{2p} \simeq \frac{1}{2p}\left[\frac{\mu^2 + \mathbf{k}_\perp^2}{x(1-x)} - \mu^2\right], \quad (5.60)
\end{aligned}
$$

where we used $|\mathbf{k}_\perp| \sim \mu \ll p$ and have introduced the decay momentum fraction x,

$$k_{1z} \equiv xp, \quad k_{1z} = (1-x)p \qquad (x \sim 1 - x \sim 1).$$

The energy difference

$$\Delta E \sim \frac{\mu_\perp^2}{x(1-x)\,p}, \qquad \mu_\perp^2 \equiv \mathbf{k}_\perp^2 + \mu^2 = \mathcal{O}\left(\mu^2\right).$$

is minimal for $x \sim \frac{1}{2}$ and can be made extremely small at high energy, $\Delta E \propto \mu^2/p$. The corresponding fluctuation time gets Lorentz dilated:

$$\Delta t \sim \frac{x(1-x)p}{\mu_\perp^2} \gg \frac{1}{\mu}. \tag{5.61}$$

Unfortunately this does not help us to achieve our goal: at high energies the decay angle decreases in the same proportion as the lifetime increases, so that the transversal displacement of the offspring remains finite,

$$|\Delta\boldsymbol{\rho}| \sim \Delta t \, |\mathbf{v}_\perp| \sim \frac{x(1-x)p}{\mu^2} \cdot \left|\frac{\mathbf{k}_\perp}{xp}\right| \sim \frac{1}{\mu},$$

the same as in (5.59b).

However, our exercise was not completely useless as we learned that at high energies long-living fluctuations may be constructed.

There is another problem with the process of (5.58). If our particle k_1 is point-like and interacts with the target 'head-on', its cross section is

proportional to the wavelength squared,

$$\sigma \sim \pi \lambda_1^2 \sim \frac{1}{k_{1z}^2} \simeq \frac{1}{(x\,p)^2} \propto \frac{1}{(x\,s)^2},$$

and falls very fast with s, unless we chose $x \sim \mu/p \ll 1$, which would take us back to the small lifetime $\Delta t \sim 1/\mu$ in (5.61)!

However, there is a way to reconcile a normal cross section with longevity. To this end we have to allow the virtual particle k_1 to decay further in order to sequentially degrade its energy. Now the particle that hits the target b has a momentum

$$p_n \sim \frac{p}{2^n}, \qquad (5.62)$$

with n the number of decays of the projectile particle a. Here we supposed, for the sake of simplicity, that in each decay the longitudinal momentum of the parent is shared equally, $x \sim \frac{1}{2}$. Now, if we reach $p_n \sim \mu$, the interaction with the target will have a normal cross section $\sigma \sim \mu^{-2}$ typical for interaction of particles with small collision energy. To get there we will have to emit

$$n \simeq \frac{\ln(p/\mu)}{\ln 2} \qquad (5.63)$$

particles. This would not have been easy if the interaction constant were small. If, on the contrary, we accept that the probability of $1 \to 2$ splittings is $\mathcal{O}(1)$ (which is not unnatural for strong dynamics), this would provide us with a realistic model of the interaction radius growing with energy.

Indeed, in the course of $n \sim \ln(s/\mu^2)$ decays a virtual particle experiences n moves in the transverse plane of the typical size $|\Delta\boldsymbol{\rho}|$ each. If emission processes are strongly correlated as shown in Fig. 5.6(a), we can get the growth as fast as

$$\rho_0(s) \sim n(s) \cdot |\Delta\boldsymbol{\rho}| \sim \frac{1}{\mu}\,\ln\frac{s}{\mu^2}. \qquad (5.64a)$$

Fig. 5.6   Correlated (a) and uncorrelated (b) motion in the $\boldsymbol{\rho}$-space.

If, on the other hand, sequential emissions are independent, as in Fig. 5.6(b), then our particle experiences a *Brownian motion* in the impact parameter space and, on the average, moves away from the origin by

$$\rho_0(s) \ \sim \ \sqrt{n(s) \cdot |\Delta\boldsymbol{\rho}|^2} \sim \frac{1}{\mu}\sqrt{\ln\frac{s}{\mu^2}}. \tag{5.64b}$$

Thus we have constructed a viable picture of how the interaction radius may become energy-dependent from the point of view of interaction dynamics.

5.6.2 Growing radius and causality

How the possibility of a growing interaction radius can be envisaged from analytic properties of the amplitude? Suppose that the factor $C(\rho, s)$ in the expression for the asymptotic of partial waves (5.46) grew as a power of energy, $C(\rho, s) \propto s^N$, so that

$$f(\rho, s) \ \simeq \ \text{const } s^N \cdot \mathrm{e}^{-2\mu\rho}, \qquad \rho \gg \mu^{-1}. \tag{5.65}$$

Recall now how the notion of the interaction radius was introduced in (5.6). Partial waves $f(\rho, s)$ are exponentially small at very large ρ. With ρ decreasing, the partial wave grows and eventually hits the saturation limit. The radius ρ_0 was defined as the value of ρ where it happens:

$$f(\rho_0, s) \simeq 8\pi \,.$$

Applying this definition to (5.65), we obtain

$$\rho_0(s) \ \simeq \ \frac{N}{2\mu}\,\ln s. \tag{5.66}$$

Formally speaking, we could have forced the radius to increase with s even faster. For example, if instead of a power we chose $C(\rho, s) \propto \exp(a\sqrt{s})$ this would have led to $\rho_0(s) \propto \sqrt{s}$.

However, such a steep growth of partial waves looks intrinsically dangerous: we know that this type of growth of the *full amplitude* $A(s, t)$ may result in the violation of causality.

It is time to reverse the logic. Let us *impose* the usual inequality that suffices to ensure causality,

$$|A(s, t)| \ \leq \ s^{N(t)} \qquad \text{for } \ s \to \infty, \tag{5.67}$$

and derive a possible growth of $\rho_0(s)$ that would dutifully respect it. Here $N(t)$ is limited in a finite interval of t (the number of necessary *subtractions* in the dispersion relation in s for a given t, see Lecture 2).

First we will take a rough model in which all partial waves with $\ell \leq \ell_0(s)$ are *saturated* while those with $\ell > \ell_0(s)$ are negligible. Then for the amplitude we have an estimate

$$|A(s,t)| \ \leq \ 16\pi \sum_{\ell=0}^{\ell_0(s)} (2\ell+1)|P_\ell(z)|\,. \tag{5.68}$$

In the $t > 0$ region we have $z = \cosh\chi > 1$, Legendre polynomials increase exponentially with ℓ, see (5.25), so that (5.68) is dominated by the last term of the sum:

$$|A(s,t)| \ \sim \ \ell_0 \, e^{\ell_0\chi_0(s)}, \tag{5.69a}$$

where, according to (5.27),

$$\chi_0(s) = \chi(t,s)\big|_{t=4\mu^2} \simeq \frac{2\mu}{k_c}, \qquad \cosh\chi(t,s) = 1 + \frac{2\,t}{s-4\mu^2}. \tag{5.69b}$$

By comparing (5.69) with (5.67) we obtain the maximal growth of the characteristic angular momentum,

$$\ell_0(s) \ \leq \ \frac{N_1}{\chi_0(s)} \ln s \ = \ k_c \cdot \frac{N_1}{2\mu} \ln s,$$

where $N_1 \equiv N(t)\big|_{t=4\mu^2}$ is the maximal number of subtractions that we need for positive t up to the first t-channel singularity at $t = 4\mu^2$.

Thus from the boundary (5.67) motivated by the causality consideration we derive two remarkable results:

$$\rho_0(s) \ \leq \ \frac{N_1}{2\mu} \ln s, \tag{5.70a}$$

$$\sigma_{\text{tot}} \ \leq \ c\ln^2 s, \qquad c = \left(\frac{N_1}{2\mu}\right)^2 \cdot \frac{\langle\text{Im}\,f\rangle}{4}, \tag{5.70b}$$

where we have used the impact parameter representation (5.56) in order to derive the upper bound for the total cross section (5.70b).

Inequalities (5.70) constitute the essence of the *Froissart theorem*.

Two remarks are in order concerning these results.

(1) Since $\text{Im}\,f$ does not exceed the unitarity limit, the coefficient c in (5.70b) is restricted by

$$c \ \leq \ \left(\frac{N_1}{2\mu}\right)^2 \cdot 4\pi.$$

(2) Moreover, we can claim that $N_1 < 2$ since otherwise we would have had among hadrons, as we shall see later, an elementary particle with spin $\sigma = 2$ and mass smaller that $2m_\pi$.

Combining these two observations we obtain

$$c \leq \frac{4\pi}{m_\pi^2} \simeq 240 \, \text{mb}.$$

5.6.3 Froissart theorem

The previous consideration was not very accurate as we arrived at (5.70) using a rough truncation of the partial-wave expansion in (5.68). Now we are ready to give a more rigorous proof of the Froissart theorem (Froissart, 1961).

We will exploit analytic properties of the elastic amplitude $A(s, z)$ as a function of the cosine of the scattering angle Θ,

$$z \equiv \cos \Theta = 1 + \frac{2\,t}{s - 4\mu^2}.$$

To prove the theorem not much is needed. It suffices to state that, as in the perturbation theory:

(1) singularities of $A(s, z)$ in z lie outside the physical region of the s-channel, $-1 \leq z \leq +1$; and in addition that

(2) for finite $|z|$ $A(s, z)$ is polynomially bounded,

$$|A(s, z)| < cs^N.$$

Then the energy growth of the interaction radius and of the total cross section is limited by (5.70). Move the integration contour $\mathcal{C}$ in the Cauchy representation,

$$A(s, z) = \frac{1}{2\pi i} \int_{\mathcal{C}} \frac{A(s, z')}{z' - z} \, dz',$$

away from the s-channel cut $-1 \leq z \leq 1$ into the unphysical region. This can always be done if there are no massless particles in the theory (in which case the t-channel singularities at $z = \pm z_0$ collide with the tips of the physical interval, ± 1). Then for the partial-wave amplitude (3.10),
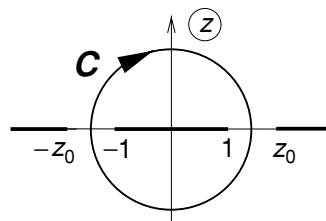
$$f_\ell(s) = \frac{1}{2} \int_{-1}^{1} dz \, A(s, z) P_\ell(z) = \frac{1}{2\pi i} \int_{\mathcal{C}} dz' \, A(s, z') Q_\ell(z'), \qquad (5.71)$$

we have a simple estimate

$$|f_\ell(s)| \; < \; \frac{L_\mathcal{C}}{2\pi} \, |A(s,z)|_{\max} \cdot |Q_\ell(z)|_{\max} \,, \qquad (5.72)$$

with subscripts max denoting maximal values of the functions on the contour, and $L_\mathcal{C}$ the length of the latter.

For $|z| > 1$ the exact boundary for the Legendre function on the contour has the form

$$|Q_\ell(z)| \; < \; c'_\ell \exp(-\ell\chi_{\min})\,, \quad \chi_{\min} \equiv \min_{z\in\mathcal{C}}\{\cosh^{-1} z\} \; \overset{s\to\infty}{\simeq} \; \frac{\sqrt{t}}{k_c}, \quad (5.73)$$

where factor c'_ℓ is non-exponential in ℓ at $\ell \to \infty$. Then (5.72) gives

$$|f_\ell(s)| \; < \; c_\ell \, s^N \exp\left\{-\frac{\ell}{k_c}\sqrt{t_{\min}}\right\}, \qquad (5.74)$$

which estimate is valid for arbitrary ℓ. So, $t_{\min}$ in (5.74) is the minimal value of t along the integration path $\mathcal{C}$. But the contour can be moved! Were it not for the cross-channel cuts $[-\infty, -z_0]$, $[z_0, +\infty]$, we could have kept 'inflating' the contour. By so doing we would *increase* $t_{\min}$ and thus strengthen the upper bound (5.74). Therefore the strongest boundary for $|f_\ell|$ that we may get is determined by the condition (5.74) with $t_{\min}$ equated with the position of the nearest singularity $t_0 = 4\mu^2$:

$$\min_{\mathcal{C}} \min_{z}\{\chi(t,s)\} = \; \cosh^{-1}\left(1 + \frac{2\,t_0}{s - 4\mu^2}\right) \implies \sqrt{t_{\min}} = \sqrt{t_0} = 2\mu.$$

The rest of the proof proceeds as above. Namely, we define $\ell_0(s)$ from the saturation condition $|f_{\ell_0}| = \text{const}$ in (5.74) and immediately obtain the maximal growth of the radius,

$$\rho_0(s) \equiv \frac{\ell_0(s)}{k_c} \; \le \; \frac{N}{2\mu} \, \ln s \; \equiv \; \rho_F(s), \qquad (5.75)$$

and of the total cross section,

$$\sigma_{\text{tot}} \simeq \frac{1}{s} \sum_{\ell=0}^{\ell_0(s)} (2\ell + 1) \, \text{Im} \, f_\ell \propto \frac{\ell_0^2(s)}{s} \; \le \; \tilde{c}\ln^2 s.$$

Let us note that the extreme Froissart regime $\rho_0 = \rho_F$ corresponds to a clear physical picture of a disc which grows fast with energy, changing neither its transparency nor the sharpness of the edge (the latter being determined by the parameter $r_0 = 1/2\mu$, see Section 5.3).

5.6.4 Pomeranchuk theorem for the case of growing radius

Now that we know that both ρ_0 and σ_{tot} may grow logarithmically, we return to the question of what can be said about the asymptotic behaviour of particle and antiparticle total interaction cross sections with a given target. Let

$$\sigma_{\text{tot}}^a = C_1 \ln^\gamma s, \quad \sigma_{\text{tot}}^{\bar a} = C_2 \ln^\gamma s, \qquad \gamma \leq 2.$$

We can easily construct the corresponding amplitudes in analogy with the case of constant cross sections considered in Section 5.5, cf. (5.51):

$$
\begin{aligned}
A_{ab}(s,0) \; &\overset{s \to \infty}{=} \; A_{\text{right}}(s) + A_{\text{left}}(-s) \\
&\simeq \frac{s\,C_1}{\pi(\gamma+1)} \ln^{\gamma+1}(-s) - \frac{s\,C_2}{\pi(\gamma+1)} \ln^{\gamma+1} s \\
&= i s \sigma_{\text{tot}}^a + \frac{s \ln s}{\pi(\gamma+1)} \cdot \Delta\sigma, \qquad \Delta\sigma \equiv \sigma_{\text{tot}}^a - \sigma_{\text{tot}}^{\bar a}.
\end{aligned}
\tag{5.76}
$$

Suppose that $C_1 \neq C_2$ ($\Delta\sigma \neq 0$). Then the imaginary part of the amplitude is relatively small and can be neglected, and not only for $t = 0$ but for finite $t < 0$ as well. The generalization of (5.76) will read

$$A_{ab}(s,t) \simeq \frac{s \ln s}{\pi(\gamma+1)} \Delta\sigma \cdot F(t,s) \tag{5.77}$$

with the factor F such that for forward scattering $F(0,s) \equiv 1$. Now we construct the differential elastic scattering cross section,

$$\frac{d\sigma_{\text{el}}}{dq^2} = \frac{1}{16\pi} \left| \frac{A(s,t)}{s} \right|^2 \simeq \frac{|F(t,s)|^2}{16\pi} \left(\frac{\Delta\sigma \ln s}{\pi(\gamma+1)} \right)^2. \tag{5.78}$$

Integration over momentum transfer gives the total elastic cross section:

$$\sigma_{\text{el}} = \int dq^2 \frac{d\sigma_{\text{el}}}{dq^2} \simeq \left(\frac{\Delta\sigma \ln s}{\pi(\gamma+1)} \right)^2 \frac{1}{16\pi} \int dq^2 |F(q^2,s)|^2. \tag{5.79}$$

The integral in (5.79) is determined by the interaction radius (see Fig. 5.4 on page 121):

$$\int dq^2 \left| F(q^2,s) \right|^2 = \frac{1}{\rho_0^2(s)}.$$

To avoid contradiction we need to impose the restriction

$$\sigma_{\text{el}} = \left(\frac{\Delta\sigma \ln s}{\pi(\gamma+1)} \right)^2 \frac{1}{16\pi\rho_0^2(s)} \leq \sigma_{\text{tot}}^a.$$

This inequality can be translated into

$$\frac{\Delta\sigma(s)}{\sigma(s)} \leq \text{const} \sqrt{\frac{\rho_0^2(s)}{\sigma(s)\ln^2 s}} = \frac{\text{const}}{\sqrt{\sigma(s)}} \cdot \frac{\rho_0(s)}{\rho_F(s)}, \qquad (5.80)$$

with ρ_F the radius corresponding to the Froissart regime (5.75).

There are two possibilities.

$\boldsymbol{\gamma = 0}$. Constant total cross sections σ_{tot}^{ab}, $\sigma_{\text{tot}}^{\bar{a}b}$. From (5.80) then follows that the asymptotic inequality $\sigma_{\text{tot}}^{ab} \neq \sigma_{\text{tot}}^{\bar{a}b}$ is possible only when $\rho_0(s) = \rho_F(s)$, that is in the case of the extreme energy growth of the radius.

$\boldsymbol{0 < \gamma \leq 2}$. Logarithmically growing cross sections:

$$\sigma = C_1 \ln^\gamma s, \qquad \Delta\sigma \leq \text{const} \, [\ln s]^{\gamma/2} \cdot \frac{\rho_0(s)}{\rho_F(s)}. \qquad (5.81)$$

In this case $C_1 = C_2$, that is the particle and antiparticle cross sections have the same asymptotic behaviour; their difference may grow with s as well though slower, with (at least) a twice smaller exponent.

In fact, it is unclear how the interaction radius $\rho_0(s)$ behaves with energy. Formally we only proved that it cannot increase faster than $\ln s$. More physical information is needed in order to choose between different regimes, e.g. $\rho \sim \sqrt{\ln s}$ and $\rho \sim \ln s$, which possibilities were offered by the picture with the number of interactions increasing with energy that we have discussed above, see (5.64).